THE EFFECT OF BOWL-IN-PISTON GEOMETRY LAYOUT ON FLUID FLOW PATTERN

by

Zoran S. JOVANOVIĆ [a*], ***Zlatomir M. ŽIVANOVIĆ*** [a], ***Željko B. ŠAKOTA*** [a], ***Miroljub V. TOMIĆ*** [b], ***and Velimir S. PETROVIĆ*** [c]

[a] Department for IC Engines and Vehicles, Vinča Institute of Nuclear Sciences, University of Belgrade, Belgrade, Serbia
[b] Department for IC Engines, Faculty of Mechanical Engineering, University of Belgrade, Belgrade, Serbia
[c] Institute IMR, Belgrade, Serbia

Original scientific paper
UDC: 621.423.3:517.96
DOI: 10.2298/TSCI110417040J

In this paper some results concerning the evolution of 3-D fluid flow pattern through all four strokes in combustion chambers with entirely different bowl-in-piston geometry layouts ranging from "omega" to "simple cylinder" were presented. All combustion chambers i. e. those with „omega" bowls, with different profiles, and those with "cylinder" bowls, with different squish area ranging from 44% to 62%, were with flat head, vertical valves, and identical elevation of intake and exhaust ports. A bunch of results emerged by dint of multidimensional modeling of non-reactive fluid flow in arbitrary geometry with moving objects and boundaries. The fluid flow pattern during induction and compression in all cases was extremely complicated and entirely 3-D. It should be noted that significant differences due to geometry of the bowl were encountered only in the vicinity of top dead centre. Namely, in the case of "omega" bowl all three types of organized macro flows were observed while in the case of "cylinder" bowl no circumferential velocity was registered at all. On the contrary, in the case of "cylinder" bowl some interesting results concerning reverse tumble and its center of rotation shifting from exhaust valve zone to intake valve zone during induction stroke and vice-verse from intake valve zone to exhaust valve zone during compression were observed while in the case of "omega" bowl no such a displacement was legible. During expansion the fluid flow pattern is fully controlled by piston motion and during exhaust it is mainly 1-D, except in the close proximity of exhaust valve. For that reason it is not affected by the geometry of the bowl.

Key words: *3-D modelling, computational fluid dynamics, fluid flow, turbulence*

Introductory remarks

Results presented in this paper are only part of a broader research concerning the mutual interaction between combustion chamber geometry layout and macro flows that incur in automotive engines. Some results related to the isolated and synergic effect of squish and

* Corresponding author; e-mail: zoranj@vinca.rs

swirl for no-valve cases are already published elsewhere [1-7] as well as results related to isolated or combined effect of the tumble in the case with 2 or 4 valves [8-20].

In the case with valves it was concluded that the idealized fluid flow pattern in the combustion chamber is the well formed high intensity tumble motion in the vicinity of the bottom dead centre (BDC). The destruction of such well formed tumble vortex in the vicinity of the top dead centre (TDC), during compression, generates the increase of turbulence intensity and larger length scale of turbulence in the vicinity of TDC yielding, for instance, in the case of IC engines, the reduction of flame kernel formation period and higher flame propagation velocity thereafter. It is coinciding with the general principle of turbulence theory which presumes that vortex filament subjected to compression reduces its length and promotes rotational velocity around its axis *i. e.* the movement is on the larger scale ("spin-up" effect).

Sooth to say the principal goal of this paper was qualitative and quantitative characterization of fluid flow through all four strokes and its analysis from the point of ideal fluid flow derogation.

Modelling of non-reactive fluid flow

The analysis of this type is inherent to multidimensional numerical modeling of non--reactive fluid flow in arbitrary geometry therefore the application of such a technique was stipulated mainly due to fact that it is the only one that encompasses the valve/port geometry in an explicit manner. In lieu of the fact that multidimensional models demands are formally constrained to initial and boundary conditions only, their application is fairly complicated and highly dependent on a set of various assumptions that are:

- 3-D conservation integral form of equations governing non-stationary turbulent flow of non-reactive compressible fluid is solved on a fine computational grid (40000-90000 cells) by dint of CGS numerical method [21-26],
- phenomenological model of turbulence was applied (RNG k-ε),
- diffusion behaves pursuant to Fick`s law,
- "wall functions" were applied for the calculation of stress tensors and heat fluxes *i. e.* boundary conditions were applied not at the wall but in its vicinity,
- Reynolds analogy was applied for heat fluxes,
- valves were treated as internal moving obstacles on a computational grid, and
- calculations were carried out for all four strokes.

Results

The analysis of the fluid flow through induction and compression stroke was carried out for combustion chambers and valve/port geometry layouts shown in figs. 1-4. Obviously, two basic combustion chamber shapes were selected and analyzed. The first one contains so called "omega" bowl in piston crown (fig. 1 and fig. 3) while the other contains cylindrical bowl (figs. 2 and 4) in piston crown. Certain variations of these basic shapes ensuing from different squish area (SA) ratios ranging from 44%-62% were generated as well but not presented here. In the case of cylindrical bowl the basic shape was not jeopardized but in the case of omega bowl the variation of squish area generated entirely new shapes due to different curvatures within the bowl. Results for variations of both basic shapes are not presented due to economy of the paper. In the case of cylindrical bowl the basic block data sheet encompasses

bore/stroke ratio *S/D* = 9.55 cm/9.843 cm, diameter of the bowl and its depth D_c = 5.6 cm and H_c = 1.155 cm, respectively, diameter of the valve D_v = 3.38 cm, squish gap *SG* = 0.2 cm and engine speed $N = 2000\ \text{min}^{-1}$. For the sake of engine compression ratio preservation in the case of cylindrical bowl the variation of SA was pursued with pertinent adjustment of geometrical parameters *i. e.* diameter and depth of the bowl and squish gap.

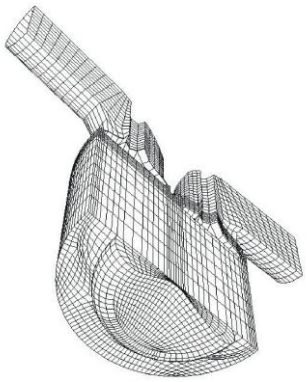

Figure 1. Perspective plot of the combustion chamber and valve/port geometry layout

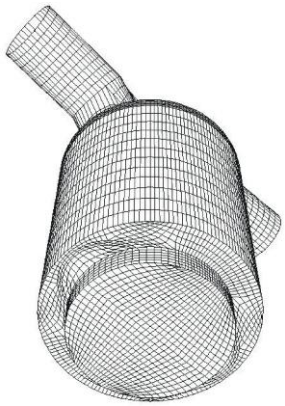

Figure 2. Perspective plot of the combustion chamber and valve/port geometry layout (*SA* = 44%, cylindrical bowl)

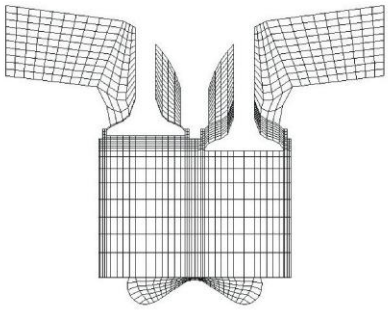

Figure 3. Combustion chamber geometry layout in x-z plane („omega“ bowl)

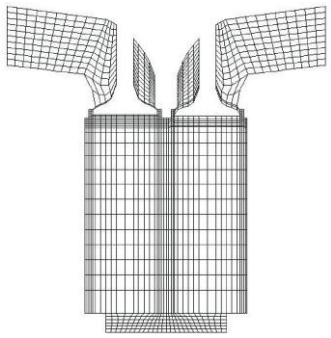

Figure 4. Combustion chamber geometry layout in x-z plane (*SA* = 44%, cylindrical bowl)

In the case of "omega" bowl the identical basic block data sheet was applied except for the profile of the bowl that was generated in a fairly arbitrary fashion. It should be stated that maximum valve lift for all cases was 0.82 cm (at 90 deg. aTDC) and the commencement of the intake valve lift was set at 15 deg. bTDC and its closure at 195 deg. aTDC. The opening of exhaust valve was set at 525 deg. aTDC and its closure at 15 deg. aTDC.

Fluid flow pattern, represented as vectors, in all three planes at the very beginning of intake stroke (15 deg. aTDC, valve lift H_v = 0.35 cm) is shown in fig. 5, 7, and 9 for "omega" bowl and figs. 6, 8 and 10 for cylindrical bowl.

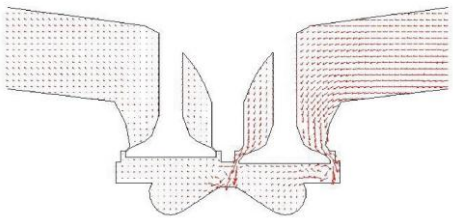

Figure 5. Fluid flow pattern in x-z plane, *y* = 0, at 15 deg. aTDC („omega" bowl)

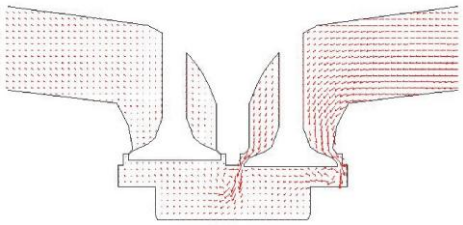

Figure 6. Fluid flow pattern in x-z plane, *y* = 0, at 15 deg. aTDC (*SA* = 54%, cylindrical bowl)

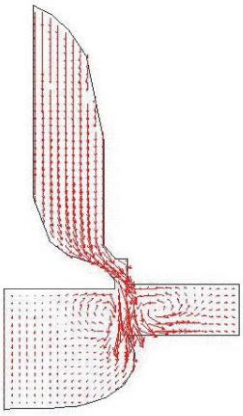

Figure 7. Fluid flow pattern in zz plane, *x* = 2 cm, at 15 deg. aTDC (intake valve zone)

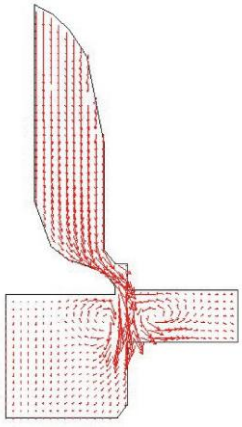

Figure 8. Fluid flow pattern in y-z plane, *x* = 2 cm, at 15 deg. aTDC (*SA* = 54%, intake valve zone)

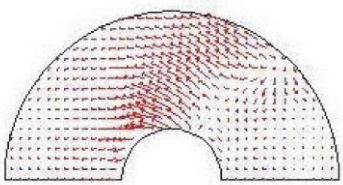

Figure 9. Fluid flow pattern in x-y plane, *x* = 9.65 cm, at 15 deg. aTDC („omega" bowl)

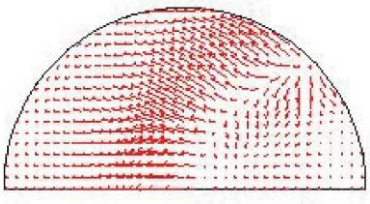

Figure 10. Fluid flow pattern in x-y plane, *x* = 9.7 cm, at 15 deg. aTDC (*SA* = 54%)

It can be seen in figs. 5 and 6 that intake flow hits the piston crown, curls and commences slightly to form the vortex flow around y-axis in a clockwise direction. At the same time the intake flow strikes upon the cylinder wall, rebounds and commences to form the vortex flow around y = const. axis in the same direction *i. e.* non-symmetric fluid flow pattern is encountered. Fairly interesting results are obtained in figs. 7 and 8 with fluid flow pattern in cut-plane through intake valve (y-z plane, x = 2 cm). The majority of the intake flow, due to larger distance of the cylinder wall, hits the piston crown in a squish zone and promotes fluid flow separation and forming of two vortices around the perimeter of the valve face. It is interesting to note that vortex flow encountered in the central part of the chamber gradually transforms into low intensity rotational flow (figs. 9 and 10 – fluid flow pattern in x-y plane, z = 9.65 cm). The further piston displacement downward (75 deg. aTDC), the increase of the valve lift (H_v = 0.77 cm) and subsequent increase of intake flow elevation generate in both cases the formation of reverse tumble with its center of rotation in the zone beneath the exhaust valve (figs. 11-14).

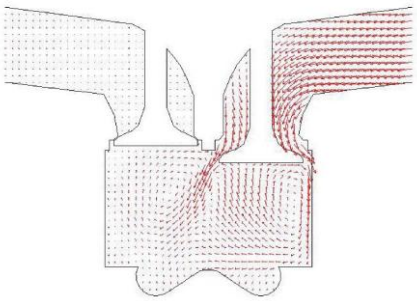

Figure 11. Fluid flow pattern in x-z plane at 75 deg. aTDC („omega“ bowl)

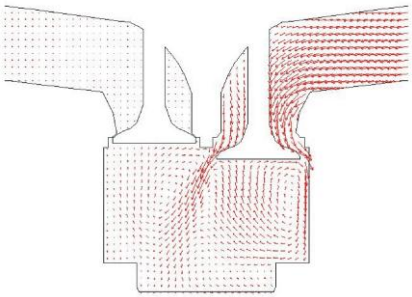

Figure 12. Fluid flow pattern in x-z plane at 75 deg. aTDC (*SA* = 54%)

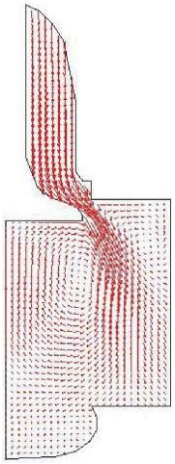

Figure 13. Fluid flow pattern in y-z plane, x = 2 cm at 75 deg. aTDC (intake valve zone, “omega” bowl)

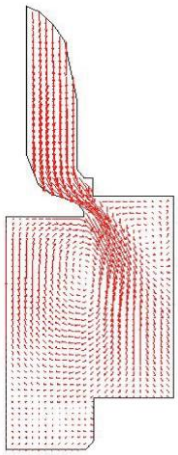

Figure 14 Fluid flow pattern in y-z plane, x = 2cm at 75 deg. aTDC (intake valve zone)

At the same time the intensity of the vortex flow in a zone between wall and valve face is increased yielding more expressive fluid flow separation, change of the fluid flow direction towards reverse tumble and intensity increase of reverse tumble thereafter.

The general increase of the zone with high intensity of turbulence is pursued with well formed vortex flow around x = const. axis. Fluid flow at the beginning of the change of direction of valve displacement (120 deg. aTDC and H_v = 0.74 cm) is characterized with conflict action of reverse tumble with its axis of rotation beneath exhaust valve and low intensity vortex flow with axis beneath intake valve. The net result is shifting of the small vortex to cylinder wall, the increase of the intensity of the reverse tumble and the displacement of its center of rotation to the central part of the chamber. The same trend is clearly legible up to 180 deg. aTDC (figs.15 and 16).

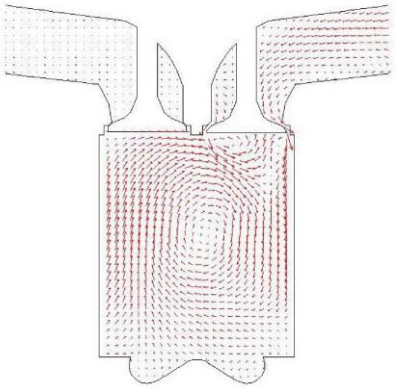

Figure 15. Fluid flow pattern in x-z plane, y = 0, at 180 deg. aTDC („omega“ bowl)

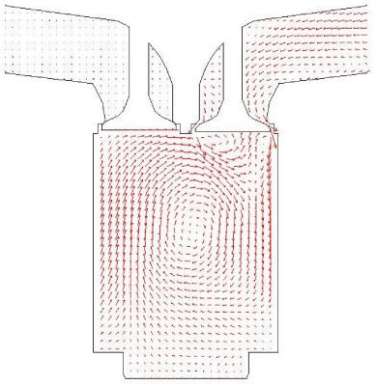

Figure 16. Fluid flow pattern in x-z plane, y = 0, at 180 deg. aTDC (SA = 54%)

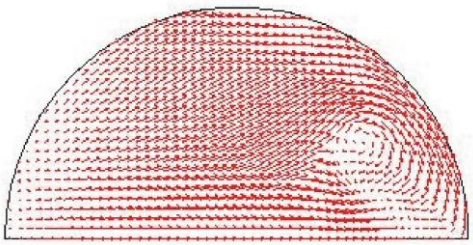

Figure 17. Fluid flow pattern in x-y plane, z = 9.65 cm, at 180 deg. aTDC („omega“ bowl)

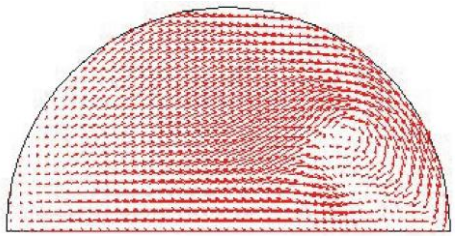

Figure 18. Fluid flow pattern in x-y plane, z = 9.65 cm, at 180 deg. aTDC (SA = 54%)

Namely, the reverse tumble increases its intensity and engulfs the central part of the combustion chamber. The axis of its rotation is shifted to the zone beneath the intake valve generating large zone with high turbulence intensity. The effect of small vortex beneath intake valve is constrained onto a small zone in the close proximity of intake valve face. The reverse tumble promotes the detention of flank vortex flows therefore only low intensity vortex flows in a cut plane passing through intake valve are encountered. Fluid flow patterns in x-y plane, z = 9.65 cm, in bDC (180 deg. aTDC, H_v = 0.15cm) immediately before intake valve closure, for “omega” and cylindrical bowls (SA = 54%) are shown in figs. 17 and 18. No legible

difference is observed. The corresponding spatial distributions of kinetic energy of turbulence (tke) in x-z plane, y = 0 and x-y plane, z = 9.65 cm for "omega" and cylindrical bowl are shown in figs. 19, 20, 21 and 22.

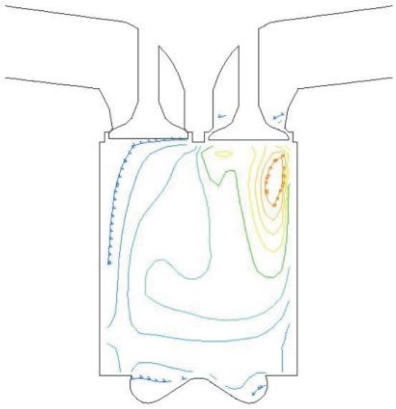

Figure 19. Spatial distribution of kinetic energy of turbulence in x-z plane, y = 0, at 180 deg. aTDC („omega" bowl)

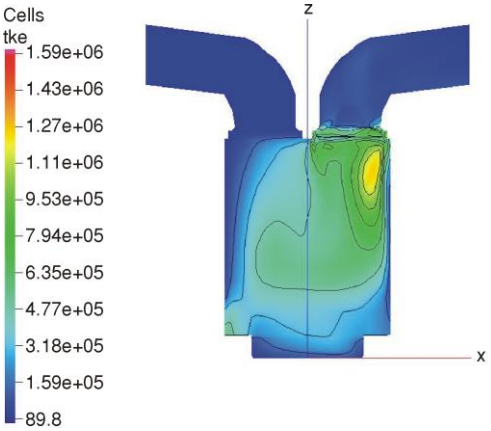

Figure 20. Spatial distribution of kinetic energy of turbulence in x-z plane, y = 0, at 180 deg. aTDC (*SA* = 54%, cylindrical bowl) (color image see on our web site)

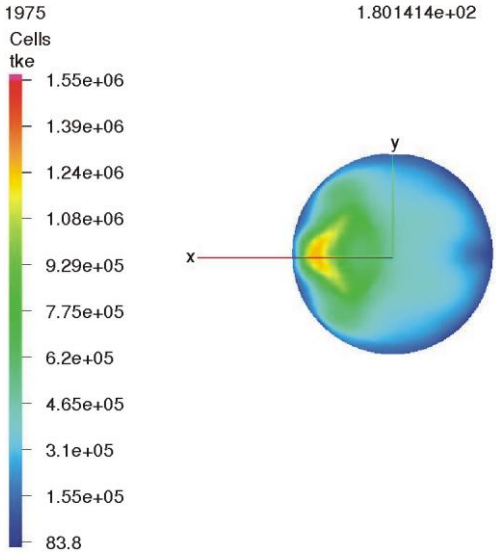

Figure 21. Spatial distribution of tke in x-y plane, z = 9.65 cm, at 180 deg. aTDC („omega" bowl) (reverse direction of x-axis) (color image see on our web site)

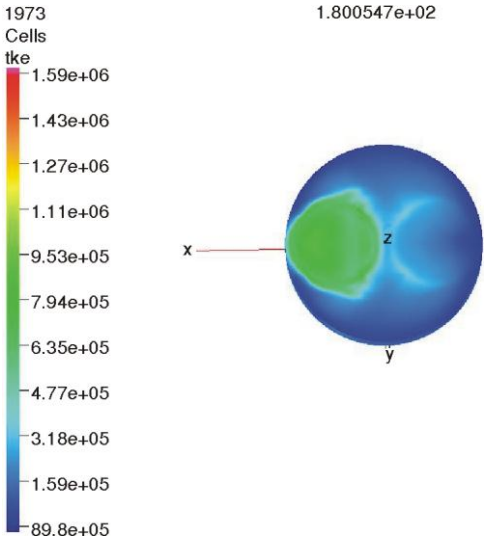

Figure 22. Spatial distribution of tke in x-y plane, z = 9.70 cm, at 180 deg. aTDC (*SA* = 54%, cylindrical bowl) (reverse direction of x-axis) (color image see on our web site)

It can be seen in fig. 15 that well formed high intensity reverse tumble engulfs the entire combustion chamber at BDC and dominates the fluid flow pattern. The gradual shifting

of reverse tumble center of rotation to the intake valve zone and the increase of its intensity affects the deflection of flank vortices and their redirection to the cylinder wall. Vortex flow in the zone beneath intake valve, to the left of its axis, is subjected to compression by dint of reverse tumble and therefore increases the velocity of its rotation. Sooth to say, in the zone beneath the intake valve the vortex flow around all three axis is encountered (fig. 17) but reverse tumble flow prevails. This explanation is verified through spatial distribution of kinetic energy of turbulence in x-z plane, $y = 0$, shown in fig. 19 and in x-y plane, $z = \text{const} = 9.65$ cm, shown in fig. 21. Obviously, the largest zone is the zone of reverse tumble effect. The effect of smaller vortices superimposed to reverse tumble flow is shown in green color while the zone with maximum turbulence intensity is designated with yellow color (zone with rotation around all three axes).

Obviously, regarding fluid flow pattern and spatial distribution of kinetic energy of turbulence, during intake stroke, there is no any difference in the case of cylindrical bowl (figs. 16, 18, 20, and 22) and "omega" bowl (fig. 15, 17, 19, and 21). Slight differences in values of kinetic energy of turbulence in figs. 21 and 22 are due to different values of $z = \text{const}$.

Fluid flow in x-z plane, during compression, is shown in fig. 23. The reverse tumble increases its intensity while the axis of its rotation gradually displaces from the central part of chamber to the intake valve zone. The higher intensity of the reverse tumble affects the destruction of the vortex beneath the intake valve, destruction of vortices in the zone between head and piston crown and decay of flank vortices with rotation around x-axis. In addition, the zone in the vicinity of piston crown is not engulfed by reverse tumble. The reverse tumble is obviously located in the central and upper part of the chamber.

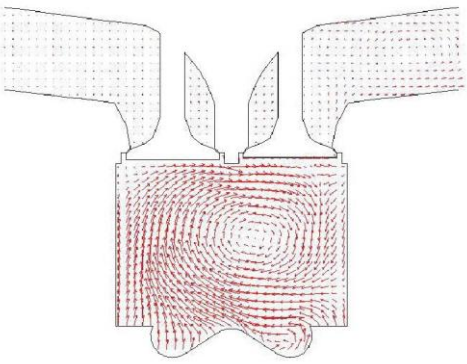

Figure 23. Fluid flow pattern in x-z plane, $z = 0$, at 270 deg. aTDC („omega" bowl)

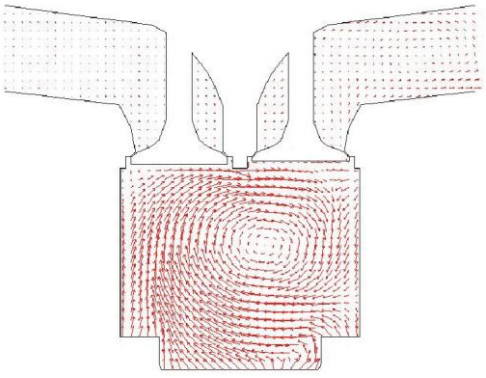

Figure 24. Fluid flow pattern in x-z plane, $z = 0$, at 270 deg. aTDC (*SA* = 54%, cylindrical bowl)

During compression the fluid flow preserves its pattern until approximately 300 deg. aTDC. Namely, as can be seen in figs. 23 and fig. 24 the location of the reverse tumble axis of rotation persists in spite of vortex motion encountered in the whole chamber due to increase of piston velocity and combustion chamber volume reduction.

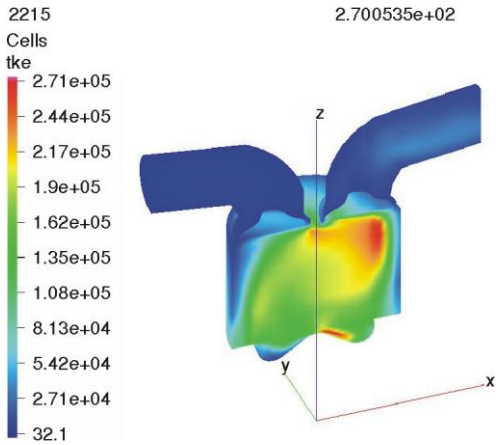

Figure 25. Perspective plot of spatial distribution of tke at 270 deg. aTDC („omega“ bowl, elevation = 35)
(color image see on our web site)

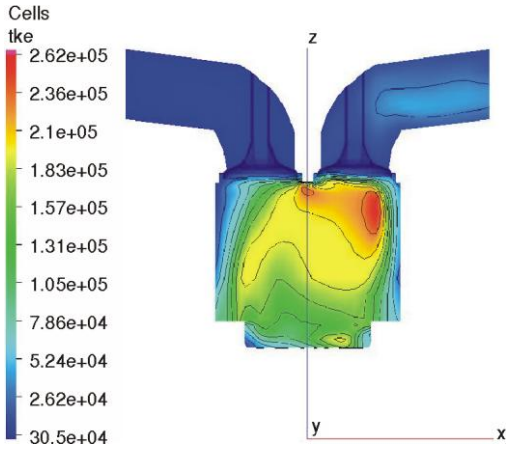

Figure 26. Spatial distribution of tke in x-z plane, *z* = 0, at 270 deg. aTDC (*SA* = 54%, cylindrical bowl)
(color image see on our web site)

At approximately 300 deg. aTDC, pursuant to “spin-up” theory, the commencement of stretching of the reverse tumble is observed yielding the engulfment of the zone beneath the exhaust valve thereafter. In the case of cylindrical bowl the reverse tumble is subjected to compression by piston movement and is slowly squeezed out from the intake valve zone. In that way the axis of its rotation is shifted to the exhaust valve (fig. 27). On the contrary the geometry of the “omega” bowl prevents such a movement (from intake to exhaust valve) therefore the entirely different motion is encountered. Namely, the reverse tumble is nearly broken up by central reef of the bowl yielding extremely complicated fluid flow composed of three clearly legible vortices in the zone beneath intake valve and two distinct vortices in the zone beneath exhaust valve (figs. 27 and 29).

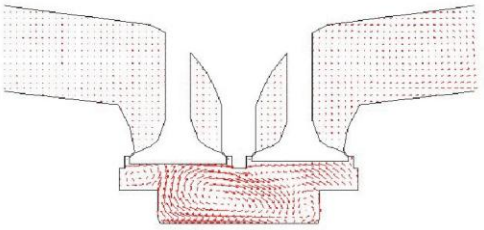

Figure 27. Fluid flow pattern in x-z plane, *y* = 0, at 345 deg. aTDC (*SA* = 54%, cylindrical bowl)

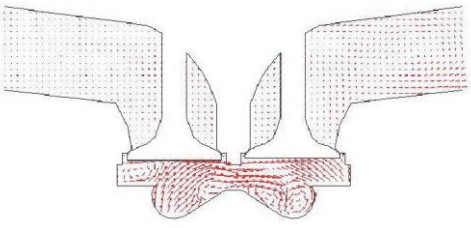

Figure 28. Fluid flow pattern in x-z plane, *y* = 0, at 345 deg. aTDC („omega“ bowl)

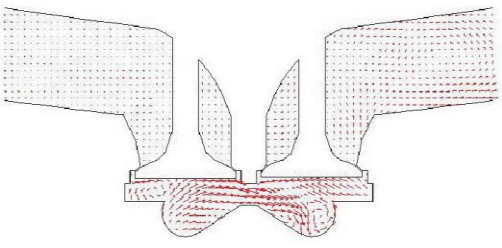

Figure 29. Fluid flow pattern in x-z plane, *y* = 0, at 360 deg. aTDC („omega“ bowl)

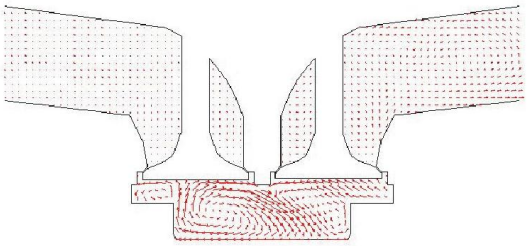

Figure 30. Fluid flow pattern in x-z plane, y = 0, at 360 deg. aTDC (*SA* = 54%, cylindrical bowl)

In the case of cylindrical bowl the same fluid flow pattern is preserved in TDC as well. Namely, in the upper part of the chamber two vortices are rotating in opposite direction (impact flow) yielding the generation of the increased coinciding flow in the zone beneath the intake valve (fig. 30).

In the case of "omega" bowl the reef in the central part of the bowl is responsible for the complete restructuring of the fluid flow. The slope of the central part of the bowl mitigates completely 3-D structure of the fluid flow in the zone beneath the intake valve converting it in well defined rotational structure shown in fig. 31. This type of macro flows was not encountered in the case with cylindrical bowl (fig. 32).

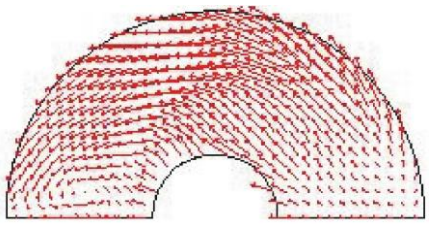

Figure 31. Fluid flow pattern in x-y plane, z = 9.65 cm, at 360 deg. aTDC ("omega" bowl)

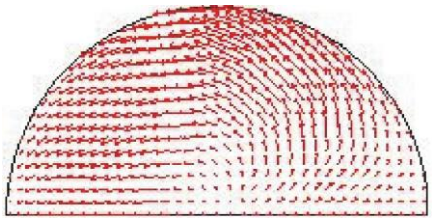

Figure 32. Fluid flow pattern in x-y plane, z = 9.65 cm, at 360 deg. aTDC(cylindrical bowl)

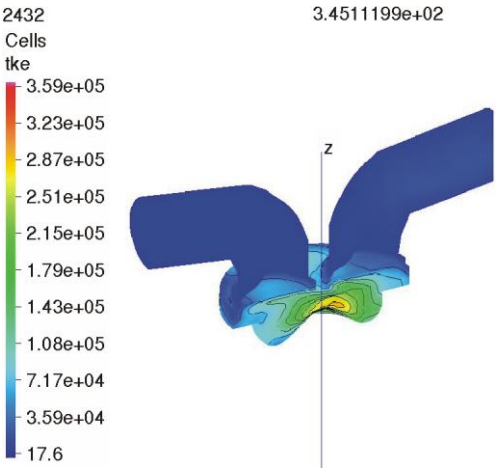

Figure 33. 3-D visualization of spatial distribution of tke at 345 deg. aTDC ("omega") (color image see on our web site)

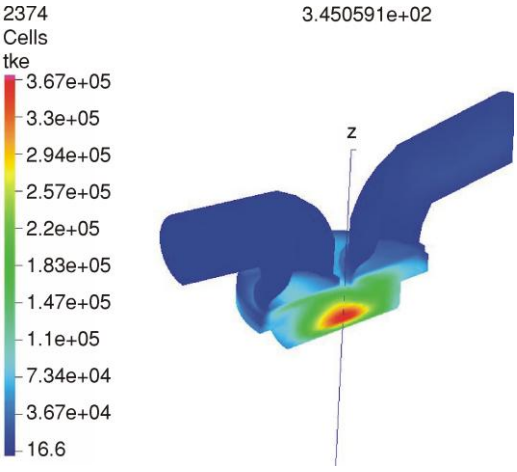

Figure 34. 3-D visualization of spatial distribution of tke at 345 deg. aTDC (cylindrical bowl) (color image see on our web site

The complicated fluid flow patterns are pursued by corresponding spatial distributions of kinetic energy of turbulence, shown in figs. 33-40.

It can be seen that the maximum kinetic energy of turbulence for the case with "omega" bowl, in TDC (360 deg. aTDC) is located in the part beneath but aside from intake valve (figs. 35 and 40) while in the case of cylindrical bowl the maximum kinetic energy of turbulence is fixed in the central part of the chamber (fig. 36).

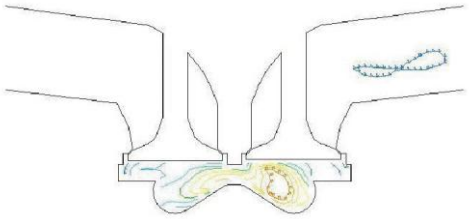

Figure 35. Spatial distribution of kinetic energy of turbulence in x-z plane, y = 0, at 360 deg. aTDC („omega" bowl)

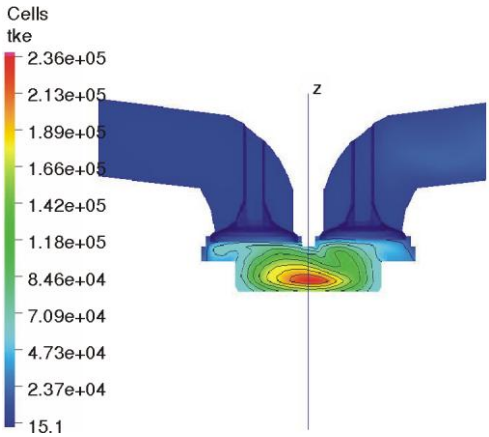

Figure 36. Spatial distribution of kinetic energy of turbulence in x-z plane, y = 0, at 360 deg. aTDC in the case of cylindrical bowl (color image see on our web site)

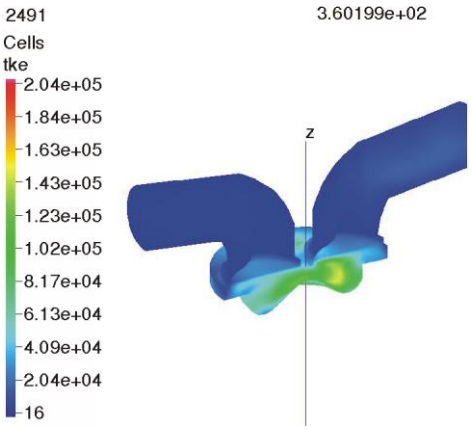

Figure 37. 3-D visualization of spatial distribution of tke at 360 deg. aTDC („omega" bowl) (color image see on our web site)

The same conclusion can be drawn out by dint of figs. 38, 39, and 40 representing spatial distribution of kinetic energy of turbulence in x-y plane for both cases. In the case of "omega" bowl the maximum kinetic energy of turbulence is, due to circumferential fluid flow that is prevailing in the space around the reef, located a little bit astray but clearly in the zone of intake valve (figs. 38 and 39). On the contrary in the case with cylindrical bowl the shifting back and forth of the centre of rotation of the reverse tumble fixes the maximum of the kinetic energy of turbulence exactly in the central part of the chamber.

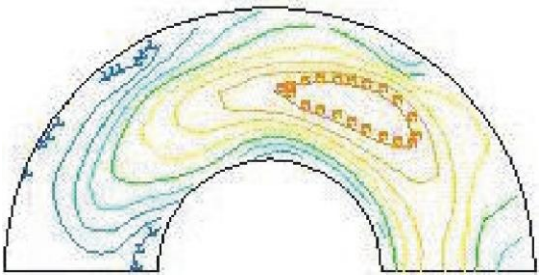

Figure 38. Spatial distribution of kinetic energy of turbulence in x-y plane, z = 9.375 cm, at 360 deg. aTDC ("omega bowl")

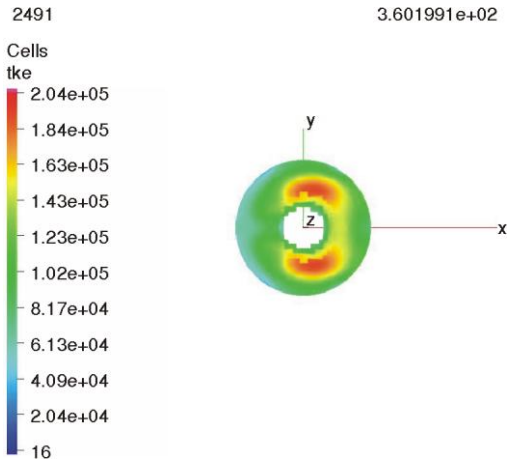

Figure 39. Spatial distribution of kinetic energy of turbulence in x-y plane, *z* = 9.65 cm, at 360 deg. aTDC ("omega" bowl)
(color image see on our web site)

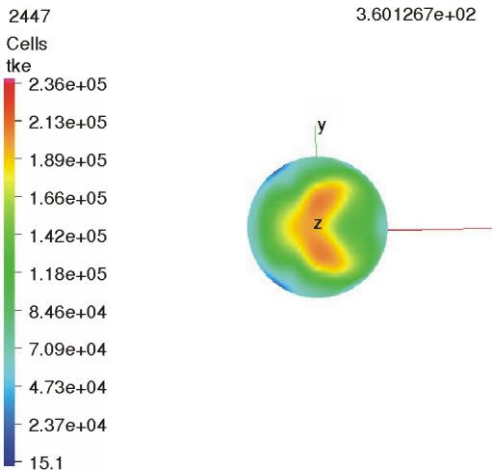

Figure 40. Spatial distribution of tke in x-y plane, *z* = 9.70 cm, at 360 deg. aTDC, cylindrical bowl
(color image see on our web site)

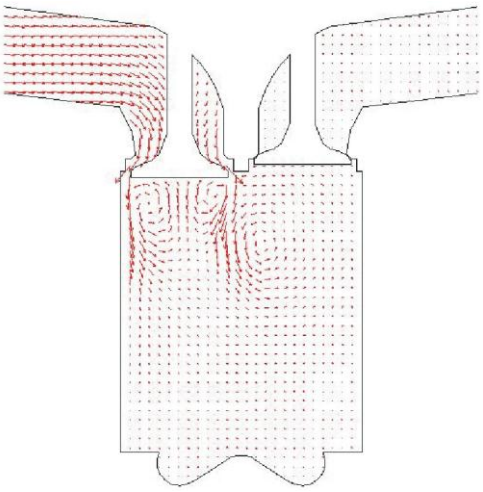

Figure 41. Fluid flow pattern in x-z plane, *y* = 0, at 540 deg. aTDC ("omega" bowl)

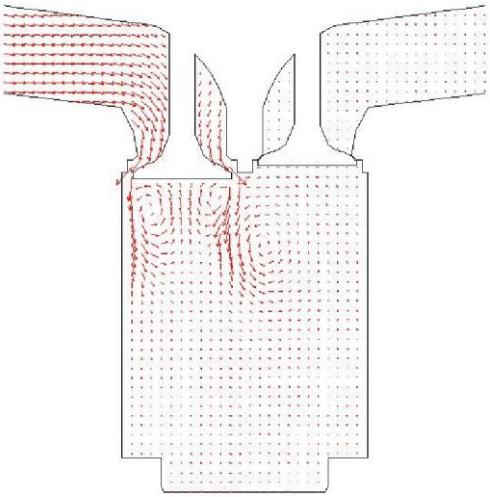

Figure 42. Fluid flow pattern in x-z plane, *y* = 0, at 540 deg. aTDC (cylindrical bowl)

During expansion rapid decay of both vortex motions is encountered. Namely laminar fluid flow is observed in the major part of the chamber both in the case of "omega" bowl (figs. 41 and 43) as well as in the case of cylindrical bowl (figs. 42 and 44). Such a fluid flow pattern is pursued by abrupt decrease of kinetic energy of turbulence (figs. 45 and 46). Some diagrams were excluded due to economy of the paper.

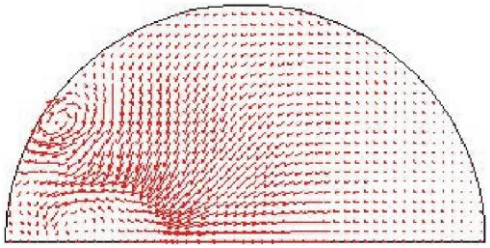

Figure 43. Fluid flow pattern in x-y plane, z = 9.65 cm, at 540 deg. ATDC („omega“ bowl))

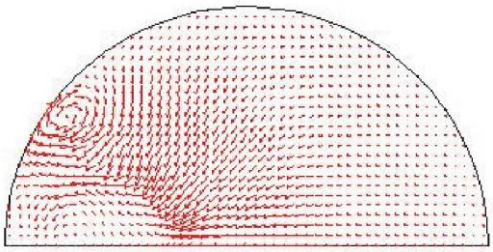

Figure 44. Fluid flow pattern in x-y plane, z = 9.70 cm, at 540 deg. aTDC (cylindrical bowl)

It is interesting to note that due to early opening of exhaust valve (525 deg aTDC) and no firing, at the very beginning of the final stroke, some ingress of fluid through exhaust valve and formation of low intensity vortex flow around all three axis is encountered (figs. 43 and 44). Low intensity level of kinetic energy of turbulence affects the location of maximum (tke) in the zone around the perimeter of the valve face (figs. 45 and 46).

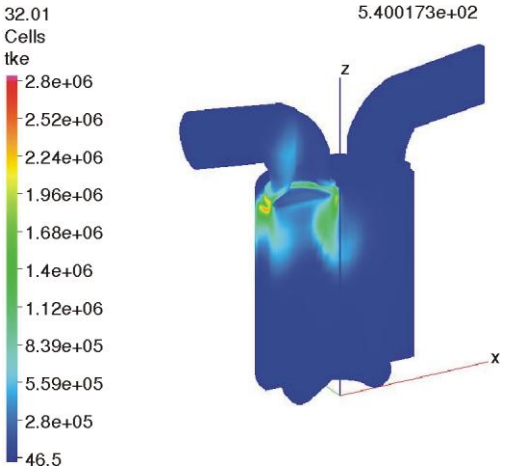

Figure 45. 3-D visualization of spatial distribution of tke at 540 deg. aTDC („omega“ bowl) (color image see on our web site)

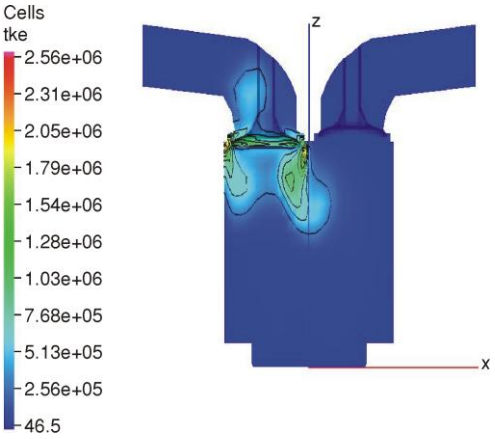

Figure 46. Spatial distribution of kinetic energy of turbulence in x-z plane, *y* = 0, at 540 deg. aTDC (cylindrical bowl) (color image see on our web site)

During final exhaust stroke the rapid decay of vortices and their subsequent transformation in laminar flow (1-D in z-axis direction) is encountered except in the close proximity of exhaust valve (figs. 47 and 48). Spatial distribution of kinetic energy of turbulence replicates entirely the fluid flow pattern (figs. 49 and 50).

Obviously no effect of the bowl shape on fluid flow pattern and spatial distribution of kinetic energy of turbulence were encountered.

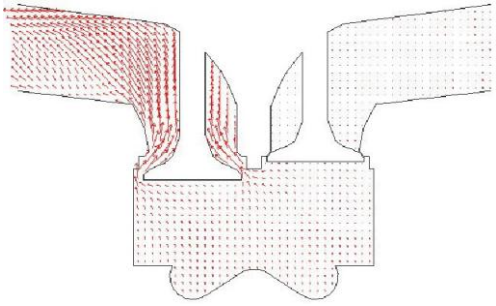

Figure 47. Fluid flow pattern in x-z plane, y = 0, at 660 deg. aTDC („omega“ bowl)

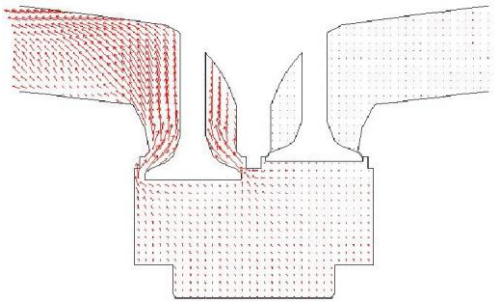

Figure 48. Fluid flow pattern in x-z plane, y = 0, at 660 deg. aTDC (cylindrical bowl)

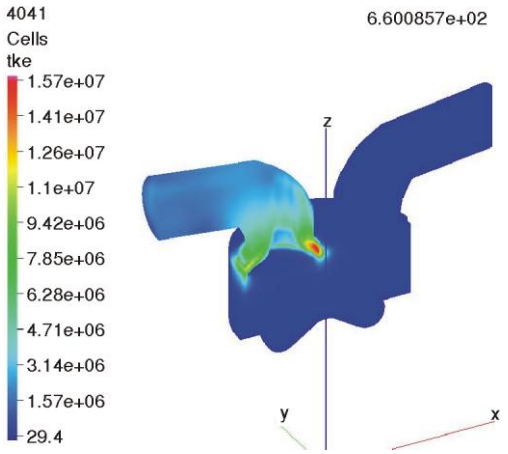

Figure 49. 3-D visualization of spatial distribution of tke at 660 deg. aTDC (“omega” bowl) (color image see on our web site)

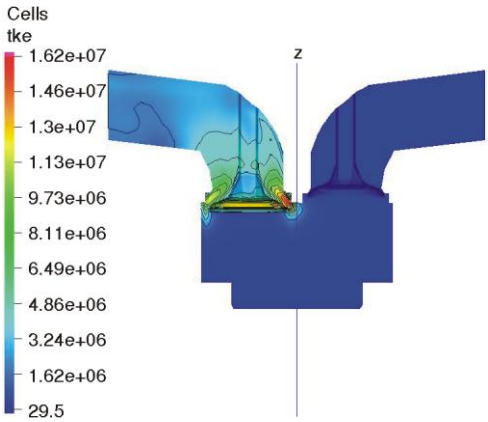

Figure 50. Spatial distribution of kinetic energy of turbulence in x-z plane, y = 0, at 660 deg. aTDC (cylindrical bowl) (color image see on our web site)

Conclusions

During intake, up to 180 deg. aTDC, fluid flow patterns and spatial distributions of kinetic energy of turbulence for both cases (“omega” and cylindrical bowl) are entirely identical. The same situation is encountered during large part of the compression stroke (up to 300 deg. aTDC). In the vicinity of TDC the fluid flow patterns pursued by spatial distributions of kinetic energy of turbulence exhibit clear differences. In the case of cylindrical bowl the characteristic back and forth shifting of axis of rotation of reverse tumble from exhaust to intake valve zone and *vice versa* is observed. In TDC, in the upper part of the combustion chamber two vortices are rotating in opposite directions (impact flow) yielding the generation of the increased coinciding flow in the zone beneath intake valve. In addition no legible vortices are seen in x-y plane. For that reason the maximum kinetic energy of turbulence is fixed in the central part of the chamber.

In the case of "omega" bowl no back and forth displacement of the axis of rotation of reverse tumble is observed but extremely complicated 3-D fluid flow composed of three clearly legible vortices in the zone beneath intake valve and two distinct vortices in the zone beneath exhaust valve. The most expressive dimensionality is concentrated primarily in the zone beneath and aside from intake valve *i. e.* in the zone with well defined circumferential flow. The maximum kinetic energy of turbulence is located in the same zone but astray due to fairly expressive circumferential fluid flow.

References

[1] Jovanović, Z., The Role of Tensor Calculus in Numerical Modeling of Combustion in IC Engines, Computer Simulation for Fluid Flow, Heat and Mass Transfer, and Combustion in Reciprocating Engines, pp. 457-541, ISBN 0-89116-392-1, Hemisphere Publishing Corporation, New York, USA, 1989

[2] Jovanović, Z., Petrović, S., Tomić, M., The Effect of Macro Flows on Flame Propagation in Combustion Chamber of IC Engines, *Proceedings*, International Symposium Science and Motor Vehicles, Belgrade, 1997, YU-97117, pp. 83-86

[3] Jovanović, Z., Petrović, S., 3-D Fluid Flow in IC Engine Combustion Chamber of Arbitrary Geometry, *Proceedings*, International Symposium MOTOAUTO 97, Russe, Bulgaria, ISBN 954-90272-2-8, Vol. II, pp.105-110

[4] Jovanović, Z., Petrović, S., The Mutual Interaction between Squish and Swirl in SI Engine Combustion Chamber, *Mobility and Vehicle Mechanics*, *23* (1997), 3, pp. 72-86

[5] Jovanović, Z., Petrović, S., The Effect of Squish Area Variation on Flame Front Shape and its Displacement, *Proceedings*, International Symposium Engine and Motor Vehicles, Kragujevac, Serbia, YU-98111, 1998

[6] Jovanović, Z., The New Fluid Flow Criterion for the Characterization of Flame Front Shape and its Displacement, *Proceedings*, 7th International Scientific Conference Simulation Research in Automotive Engineering, Lublin, Poland, 1999, pp. 1-7

[7] Jovanović, Z., The Modification of the Combustion Chamber Geometry Layout on the Basis of Fluid Flow Pattern Criteria, *Proceedings*, International Conference MOTOAUTO 99, Plovdiv, Bulgaria, 1999, pp. 31-37

[8] Chen, A., Lee, K. C., Yianneskis, M., Velocity Characteristics of Steady Flow through a Straight Generic Inlet Port, *International Journal for Numerical Methods in Fluids*, *21* (1995), 7, pp. 571-590

[9] Nadarajah, S., Tindal, M. J., Yianneskis, M., Swirl Centre Precession under Steady Flow Conditions, *Proceedings* of the Institution of Mechanical Engineering, Part D, London, C413/065, pp. 103-108, 1991

[10] Jovanović, Z., Petrović, S., The Effect of Intake Flow Modeling on Flame Front Shape and its Displacement in Cylindrical Combustion Chamber, Society of Automotive Engineers, SP Publication, Multidimensional Engine Modeling, Detroit, Mich., USA, 2001, pp. 1-6

[11] Jovanović, Z., The Displacement of the Reverse Tumble Centre of Rotation during Induction and Compression, *MVM*, *26* (2000), 1-2, pp. 29-44

[12] Jovanović, Z., Petrović, S., The Effect of Tumble on Flame Front Shape and its Displacement, *Proceedings*, International Symposium Automotive and Environment, Pitesti, Romania, 2000, pp. 153-159

[13] Jovanović, Z., The Mutual Interaction between Squish and Tumble in Combustion Chamber with Cylindrical Bowl, *Inernational Journal for Vehicle Mechanics, Engines and Transportation System, Mobility and Vehicle Mechanics*, *27* (2001), 1-2, pp. 19-32

[14] Jovanović, Z., Basara, B., The Structure of Intake Flow in 4-Valve Engines, International Automotive Conference Science & Motor Vehicles, YUMV 01022, Belgrade, 2001, pp. 97-100

[15] Basara, B., Jovanović, Z., The Current Capabilities of Turbulence Modeling in Automotive Flows, International Automotive Conference Science & Motor Vehicles, YUMV 010021, Belgrade, 2001, pp. 93-96

[16] Jovanović, Z., 3-D Modeling of Nonreactive Fluid Flow in a Particular Combustion Chamber, *Proceedings*, International Scientific Meeting Motor Vehicles and Engines, MVM04-B21, Kragujevac, Serbia, 2004, pp. 551-562

[17] Jovanović, Z., Tomić, M., Modeling of Non-Reactive Fluid Flow in a Diesel-Like Combustion Chamber, International Congress Motor Vehicles & Motors, Kragujevac, Serbia, MVM20060068, 2006, pp. 551-562
[18] Masoničić, Z., Jovanović, Z., The Effect of Combustion Chamber Geometry Layout Variations onto Fluid Flow Pattern, International Automotive Conference Science $ Motor Vehicles, Belgrade 2007 – Paper NMV0774, ISBN 978-86-80941-31-8
[19] Jovanović, Z., Masoničić, Z., Tomić, M., The Vice-Verse Movement of the Reverse Tumble Center of Rotation in a Particular Combustion Chamber, *MTM Machines Technologies Materials, International virtual Journal for Science, Technics and Innovations for the Industry*, *2* (2008), 6-7, pp. 17-20
[20] Jovanović, Z., Basara, B., The Controversy Concerning Turbulence Modeling in Automotive Application, PCO Global Conference, Kuching, Sarawak, Borneo, Malaysia, 2010, Paper M13, ISBN 978-983-44483-32
[21] Jovanović, Z., Petrović, S., Tomić, M., The Effect of Combustion Chamber Geometry Layout on Combustion and Emission, *Thermal Science*, *12* (2008), 1, pp. 7-24
[22] Gosman, A. D., Flow Processes in Cylinders, The Thermodynamics and Gas Dynamics of IC Engines, Oxford Science Publications, ISBN 0-19-856212-8, 1986, Vol. II, pp. 616-772
[23] Amsden, A. A., KIVAII: A Computer Program for Chemically Reactive Flows with Sprays, LA-11560-MS,1989
[24] Amsden, A. A., KIVA3V, Rel.2-Improvements to KIVA3V, LA-UR-99-915, 1999
[25] Amsden, A. A., SALE3D: A Simplified ALE Computer Program for Calculating 3-D Fluid Flows, NUREG-CR-2185, 1982, 11560-MS, 1989
[26] Torres, D. J., Trujillo, M. F., KIVA-4: An Unstructured ALE Code for Compressible Gas Flow with Sprays, *Journal of Computational Physics*, *219* (2006), 2, pp. 943-975

Paper submitted: April 15, 2011
Paper revised: May 4, 2011
Paper accepted: May 4, 2011